



AALBORG UNIVERSITY
DENMARK

Aalborg Universitet

Load Torque Compensator for Model Predictive Direct Current Control in High Power PMSM Drive Systems

Preindl, Matthias; Schaltz, Erik

Published in:
Journal of Energy and Power Engineering

Publication date:
2011

Document Version
Tidlig version også kaldet pre-print

[Link to publication from Aalborg University](#)

Citation for published version (APA):
Preindl, M., & Schaltz, E. (2011). Load Torque Compensator for Model Predictive Direct Current Control in High Power PMSM Drive Systems. *Journal of Energy and Power Engineering*, 5(6), 554-561.

General rights

Copyright and moral rights for the publications made accessible in the public portal are retained by the authors and/or other copyright owners and it is a condition of accessing publications that users recognise and abide by the legal requirements associated with these rights.

- Users may download and print one copy of any publication from the public portal for the purpose of private study or research.
- You may not further distribute the material or use it for any profit-making activity or commercial gain
- You may freely distribute the URL identifying the publication in the public portal -

Take down policy

If you believe that this document breaches copyright please contact us at vbn@aub.aau.dk providing details, and we will remove access to the work immediately and investigate your claim.

Load Torque Compensator for Model Predictive Direct Current Control in High Power PMSM Drive Systems

M. Preindl^{1,2} and E. Scholtz²

1. Power Electronic Systems Laboratory, ETH Zurich, Zurich 8092, Switzerland

2. Department of Energy Technology, Aalborg University, Aalborg 9220, Denmark

Received: September 02, 2010 / Accepted: December 10, 2010 / Published: June 30, 2011.

Abstract: The widely used cascade speed and torque controllers have a limited control performance in most high power applications due to the low switching frequency of power electronic converters and the convenience to avoid speed overshoots and oscillations for lifetime considerations. Model Predictive Direct Current Control (MPDCC) leads to an increase of torque control performance taking into account the discrete nature of inverters but temporary offsets and poor responses to load torque variations are still issues in speed control. A load torque estimator is proposed in this paper in order to further improve dynamic behavior. It compensates the load torque influence on the speed control setting a feed forward torque reference value. The benefits are twice; the speed controller reaches the speed reference value without offsets which would need to be compensated by an integrator and a better response to load torque variations is obtained since they are detected and compensated leading to small speed variations. Moreover, the influence of parameter errors and disturbances has been analyzed and limited so that they play a minor role in operation.

Keywords: Drive systems, model predictive control (MPC), current control, switching frequency optimization.

1. Introduction

The most popular structure for electrical machine speed control is the cascade structure and it is widely used in industry. Applied to the Permanent Magnet Synchronous Machine (PMSM), it contains an inner current i.e. torque control loop and an outer speed control loop. In order to obtain stability the bandwidth of the current control loop must be limited according to the sampling frequency of the system. For the same reason the control action of the control loops is decoupled to further reduce the speed control bandwidth and design the speed control action slower than of the current control one. Moreover a safety margin should be introduced in order to obtain control robustness.

The machine speed controller has the assignment to minimize the difference between the speed reference

and the actual speed. Depending on the application the speed control performance can be very poor, above all in high power systems where the sampling and switching frequency is in the order of e.g. 1 kHz.

Assuming the use of linear controllers, the rise time on e.g. a reference step can be improved using an aggressive tuning. On the other hand such a design leads to oscillations and overshoots and they can lead to problems. Mechanical parts of the system are stressed, which reduces the lifetime, and hardware protections can be irritated. Oscillations in speed are also reported in the absorbed or injected power which is not desired in power generators like wind turbines.

For this reason, less aggressive control is preferred in many applications where speed dynamics is not crucial. On the other hand, the compensation of the load torque is part of the speed control, where it is seen as a control disturbance (Fig. 1). Assuming proportional control action it introduces an offset in speed. This offset is usually compensated by the

Corresponding author: M. Preindl, M.Sc., R&D Engineer, research fields: power electronic converters, drive systems, and wind power. E-mail: matthias.preindl@gmail.com.

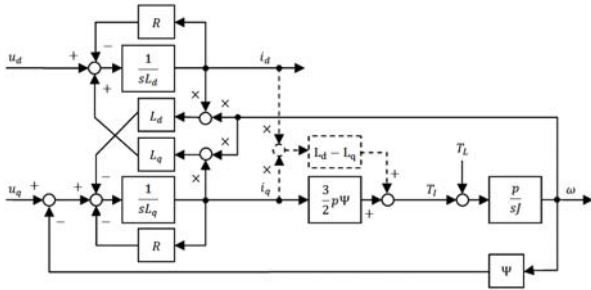


Fig. 1 Block diagram of the PMSM.

integration part of the controller using relatively high gains. However, the compensation do not work well if those gains must be limited to reduce aggressiveness and the compensation of e.g. a constant offset due to a constant load torque is slow.

However, the load torque can be compensated with a feed-forward term setting a torque, i.e. current reference value with a load torque estimator. In this structure, the speed controller looks after its main duty: the speed control actions are independent from the load torque.

Load torque compensators have been proposed in literature based on Kalman filters [1, 2], adaptive control [3], neural networks [4-6], etc. However, execution time of such structures can be fairly long and in current control approaches which do not use modulation schemes (like MPDCC) the execution time is already a critical issue. For this reason a fast but possibly less accurate solution is preferred.

The load torque dependences can be obtained from the PMSM model and computed with the available measurements. However, disturbances are expected above all in the range of the sampling and switching frequency due to the MPDCC control concept, which is based on instantaneous values. Suitable feed-forward values can be obtained using a first-order filter, which limits also the bandwidth of structure according to the cascade control demands.

The compensated speed control loop has been combined with an inner Model Predictive Current Direct Control (MPDCC) current controller (similar concepts are also called Predictive Direct Control [7] or Finite Control Set Model Predictive Control [8]). It

takes into account the discrete states of the inverter [9, 10] and the future behavior is predicted based on a load model [11, 12] in discrete time steps.

A cost function (known also as quality or decision function) [13] provides the criterion for choosing the appropriate control action. The prediction sequences are evaluated with the aid of the cost function, and the one minimizing the cost function is selected. The MPDCC cost function can be optimized according to the application in question and the goal can be to increase the control dynamics [7] or to reduce the switching frequency obtaining a certain torque ripple [14, 15].

The definition of the observer and feed-forward structure is shown in Chapter 2. In Chapter 3 the analysis of the estimator is presented in order to evaluate the estimation bandwidth and the disturbance dependence. The used MPDCC current control structure is shown in Chapter 4 and the simulation and experimental results for the observer and the sensorless MPDCC are presented in Chapter 5.

2. Definition

In this section the load torque observer is defined and its application to the speed control loop as feed-forward path is shown.

2.1 Load Torque Estimation

The speed torque dependences are obtained with the PMSM model which is shown in Fig. 1. J is the moment of inertia, p the number of pole pairs, ω the electrical speed, T_e the electromagnetic torque, and T_l the load torque.

$$\frac{J}{p} \frac{d\omega}{dt} = T_e - T_l \tag{1}$$

Thus the electromagnetic torque is given by the following equations, where the friction torque is part of the load torque. For the following equations a round-rotor or small saliency PMSM is assumed, where the reluctance torque can be neglected. The parameter ψ is the permanent magnet flux.

$$T_e = \frac{3}{2} p \psi i_q \quad (2)$$

$$T_e = T_l + \frac{J}{p} \frac{d\omega}{dt} \quad (3)$$

The estimator should be used to provide a feed-forward value in the speed controller in order to decouple the load torque from the speed control. The electromagnetic torque is divided in a feed-forward value T_{eT_l} which should compensate the load torque T_l , and a dynamic value $T_{e\Delta\omega}$ which takes account of the speed variation.

$$T_e = T_{eT_l} + T_{e\Delta\omega} = T_l + \frac{J}{p} \frac{d\omega}{dt} \quad (4)$$

$$T_{eT_l} = T_l \quad (5)$$

$$T_{e\Delta\omega} = \frac{J}{p} \frac{d\omega}{dt} \quad (6)$$

Therefore the speed controller provides $T_{e\Delta\omega}$ for speed control and the feed-forward path provides T_{eT_l} for load torque compensation. However, the electrical torque is not directly known, but it is proportional to the q -axis current and can be calculated. The load torque can be estimated with the calculated electrical torque and the variation of the machine speed.

$$\hat{T}_l = T_{eT_l} = T_e - T_{e\Delta\omega} = \frac{3}{2} p \psi i_q - \frac{J}{p} \frac{d\omega}{dt} \quad (7)$$

2.2 Filter Structure

The disturbance dependence of the estimate \hat{T}_l can be reduced using a filter. In order to achieve the required fast execution time a first order filter has been used. It is designed to reduce disturbances frequencies in the order of the sampling frequency.

In the literature many filter structures can be found, a fairly convenient for discrete filtering is shown in this section. It is a first order filter structure and is mainly employed for estimation issues.

The principle of this structure is the calculation of the error, i.e. difference between the actual value $\hat{T}_l[k]$ and the last filtered value $\hat{T}_l[k-1]$.

$$e[k] = \hat{T}_l[k] - \hat{T}_l[k-1] \quad (8)$$

The filtered value is generated by integration of the error, i.e. the error is used to update the output value.

Integration means in the discrete domain summation and multiplication with the sampling period T_s . \hat{T}_l is the filtered value and ω_f is a coefficient which determines the bandwidth of the structure.

$$\hat{T}_l[k] = \omega_f T_s \sum_{i=0}^k e[i] \quad (9)$$

2.3 Feed-Forward Term

The speed controller sets the torque indirectly by giving a current reference value on the q -axis. For this reason the estimator has to provide the reference current $i_{qT_l}^*$ which is added to the PI-controller output $i_{q\Delta\omega}^*$ i.e. the total reference current is $i_q^* = i_{qT_l}^* + i_{q\Delta\omega}^*$.

$$i_{qT_l}^*[k] = \frac{\hat{T}_l[k]}{\frac{3}{2} p \psi} \quad (10)$$

The structure of the modified speed controller, i.e. the P controller with feed-forward path is shown in Fig. 2. Moreover the block diagram of the load torque, i.e. the feed-forward path structure is shown.

The maximum current and the corresponding maximum torque is limited at the controller output i_q^* to its nominal value.

3. Observer Analysis

The transfer functions are important to analyze the observer and filter behavior. Moreover the bandwidth and the disturbance dependence of the observer can be derived.

The equivalent circuit in Fig. 3 can be used for the observer analysis. The d -axis current control is not shown since it does not influence the torque control in round rotor and small saliency PMSM. Moreover the current control loop is substituted with a first order pole with the cutoff frequency equal to its bandwidth and models effects below its bandwidth with good approximation.

3.1 Observer Bandwidth and Stability

The load torque observer behavior can be described by the transfer function $G_{\hat{T}_l T_l}(s)$, which is shown in Fig. 4.

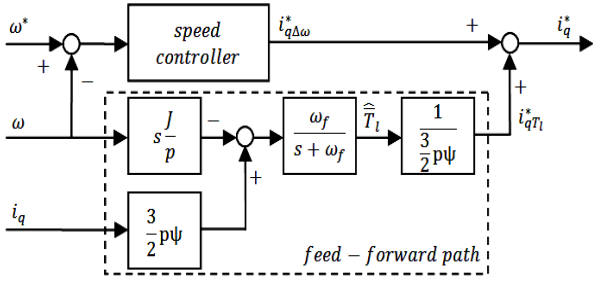


Fig. 2 Speed control structure with feed-forward path.

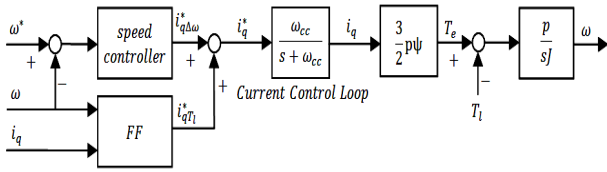


Fig. 3 Block diagram of the control and the plant. The current control loop is substituted with a first order pole which models effects below its bandwidth with good approximation.

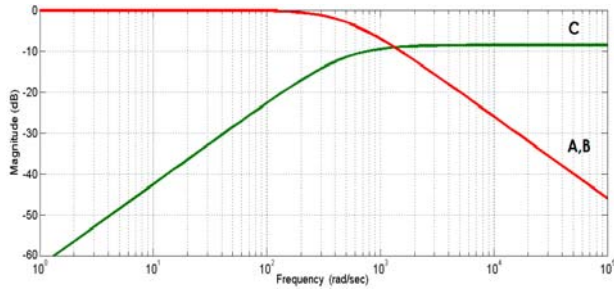


Fig. 4 Observer transfer functions: $G_{\hat{T}_l T_l}(s)$ (A), $G_{i_q T_l i_q}(s)$ (B), and $G_{i_q T_l \omega}(s)$ (C). The transfer function have been plotted with the parameters: $\omega_f = 500 \text{ rad/s}$, $J = 5e-3 \text{ kgm}^2$, $p = 3$, $\psi = 0.495 \text{ Wb}$.

$$G_{\hat{T}_l T_l}(s) = \frac{\hat{T}_l}{T_l} = \frac{1}{\frac{s}{\omega_f} + 1} \quad (11)$$

In order to meet stability and robustness criteria, the feed-forward value should not act with a larger bandwidth than speed controller. For this reason the factor ω_f which sets the bandwidth must be chosen accordingly.

3.2 Disturbance Dependence

The disturbance dependence can be evaluated with the transfer functions between the inputs and output of the estimator which are shown in Fig. 4. Since the load torque is compensated by setting a current reference the

influence of disturbances on this value is shown.

$$G_{i_q T_l i_q}^*(s) = \frac{i_q^* T_l}{i_q} = \frac{1}{\frac{s}{\omega_f} + 1} \quad (12)$$

$$G_{i_q T_l \omega}^*(s) = \frac{i_q^* T_l}{\omega} = \frac{J}{\frac{3}{2} p \psi} \frac{s}{\omega_f} + 1 \quad (13)$$

The disturbances at the input i_q are suitable for the feed-forward term since the value is also used as feedback in the current control loop. On the other hand the output is potentially sensitive to high frequency disturbances at the input ω due to the derivation. However with the first order filter the gain of the transfer function is limited and remains always below 1, i.e. disturbances are not amplified.

3.3 Parameter Dependence

The observer is based on model inversion and for this reason it is also parameter dependent. The filter can be ignored for the frequency bandwidth below its bandwidth. The transfer functions can be rewritten for this case.

$$G_{i_q T_l i_q}^*(s) = \frac{i_q^* T_l}{i_q} = 1 \quad (14)$$

$$G_{i_q T_l \omega}^*(s) = \frac{i_q^* T_l}{\omega} = s \frac{J}{p \frac{3}{2} p \psi} \quad (15)$$

According to the transfer functions parameter variations can distort only the ω input. Influence is expected during transients since output according to this value is zero at steady state. Variations are expected eventually on the values J and ψ . A positive overall variation, e.g. +20%, leads to a negative offset in the applied electromagnetic torque during speed transients and vice versa. This offset must be compensated by the speed controller.

4. Introduction to MPDCC

MPDCC uses a simple modulation concept instead of a modulation scheme like PWM or SVM. Model predictive control is used in order to take the future

behavior of the inverter into account. Optimal current control is desired but it can only be obtained with respect to a cost function. The main challenge besides developing the control structure itself is to find a proper cost function. The design and implementation of the MPDCC controller is shown in the dq -reference frame in this section.

4.1 Current Error Prediction

For a given inverter state, i.e. output voltage and the current error $e[k] = \underline{i}^*[k] - \underline{i}[k]$ the current error of the next sampling period $e[k+1]$ based on the load model can be predicted. Applying the calculation on each state vector, the one which is most convenient due to the cost function can be chosen.

The difference between the reference and actual current vector is defined as error on both axis. The current reference value \underline{i}^* is seen to be unpredictable and thus assumed to be constant. \underline{i} is the current vector and e the current error. The indices d, q refer to the reference frame axes respectively.

$$e_d[k] = i_d^* - i_d[k] \quad (16)$$

$$e_q[k] = i_q^* - i_q[k] \quad (17)$$

The current and thus its error can be modified by applying a voltage vector. For this reason the influence of each vector on the current can be predicted in order to choose the one with the expected effect. The basis for the prediction is the load model. R is the stator resistance, L is the inductance, $\underline{u}_{0..7}$ the inverter voltage depending on the states 0–7, ψ the flux generated by the permanent magnets, and ω the electrical angular velocity.

$$\underline{u}_{d0..7} = L_d \frac{di_d}{dt} + Ri_d - \omega L_q i_q \quad (18)$$

$$\underline{u}_{q0..7} = L_q \frac{di_q}{dt} + Ri_q + \omega L_d i_d + \omega \psi \quad (19)$$

The current driving voltage, i.e. the voltage on the inductances \underline{u}_L depends on the applied inverter state, the resistive voltage drop, the cross coupling between the two axis and the back-emf.

$$\underline{u}_{Ld} = L_d \frac{di_d}{dt} = \underline{u}_{d0..7} - Ri_d + \omega L_q i_q \quad (20)$$

$$\underline{u}_{Lq} = L_q \frac{di_q}{dt} = \underline{u}_{q0..7} - Ri_q - \omega L_d i_d - \omega \psi \quad (21)$$

Over a defined time the expected current change can be calculated by integration, which depends above all on the applied inverter state vector. The time which the voltage is applied is the sampling time period T_s . The changes in i_d and i_q are given by:

$$\Delta i_d[k+1] = \left(\underline{u}_{d0..7}[k] - Ri_d[k] + \omega[k]L_q i_q[k] \right) \frac{T_s}{L_d} \quad (22)$$

$$\Delta i_q[k+1] = \left(\underline{u}_{q0..7}[k] - Ri_q[k] - \omega[k]L_d i_d[k] - \omega[k]\psi \right) \frac{T_s}{L_q} \quad (23)$$

Thus the current and its error can be predicted with the assumption of constant reference currents.

$$e_d[k+1] = e_d[k] - \Delta i_d[k+1] \quad (24)$$

$$e_q[k+1] = e_q[k] - \Delta i_q[k+1] \quad (25)$$

4.2 Graph Algorithm

The prediction of all eight possible errors is time demanding and not necessary. Supposing to be in an inverter state it is not necessary to have the possibility to switch all possible inverter states in the next sampling period in order to control the current. It is enough to be able to switch the two neighbor vectors and a zero vector, which are obtained by changing one leg state. However if the actual state is a zero vector, all active vectors must be reachable in order to avoid spikes in the current ripple.

The graph algorithm leads to another advantage: the number of leg state changes per sampling period is limited. Thus, the switching frequency depends only on the number of vector changes, i.e. inverter state changes and its restriction can eventually be part of the control algorithm. The possible paths are shown in the graph diagram in Fig. 5.

4.3 Cost Function

In order to achieve high dynamics, the goal is to minimize as fast as possible the current error and the voltage vector which lead to the smallest predicted error, i.e. reduces best the error should be chosen. For this reason a cost function is designed depending on the

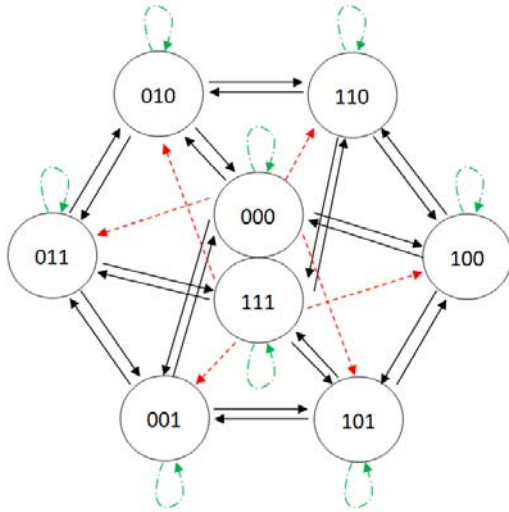


Fig. 5 Inverter state graph: paths show the possible changes. Double dashed line: no switching, continuous line: one state change and for the dashed-line: two state changes are necessary. The states e.g. 100 refer to the switching state of each inverter leg, where 1 means the upper transistor is on and the lower one is off and 0 indicates inverse switching states.

predicted current error and the vector with the smallest cost will be applied. Furthermore a steady state switching frequency reduction is possible but it is not shown in this paper.

The cost function is the criteria of which vector, i.e. output voltage will be applied to the load. For each vector the cost is calculated and the cheapest one will be chosen. If a vector should not be applied due to the graph its cost is set to a high value and thus it will not be chosen.

Since the goal is to minimize the current error, the voltage vector which application lead to the smallest predicted error in the next sampling period is chosen. The cost function is:

$$c_{0..7} = (e_d[k+1])^2 + (e_q[k+1])^2 \quad (26)$$

5. Results

The load torque observer has been simulated and tested experimentally on a 3 pole PMSM. The parameters are 310V inverter dc-voltage, 3.7A nominal current, 30mH and 38mH d and q inductance respectively, and 0.495Wb flux generated by the permanent magnets. Since MPDCC is typical for

drive systems with higher power ratings, the switching frequency has been limited to 5kHz (worst case).

The speed controller was designed as simple as possible in order to show the potential of the feed-forward structure: a P-controller. With this controller can be made sure to not obtain overshoots and oscillations. Moreover the P controller with feed forward path is compared to a PI controller.

5.1 Speed Reference Steps

Three speed reference steps have been applied to the drive system in order to show the speed control properties. The simulation speed reference step results are shown in Fig. 6 and the corresponding experimental results are shown in Fig. 7.

Using a PI controller lead without load torque to an overshoot which is dropped by the integrator. However applying a constant load torque the proportional part of the controller accelerates the machine until it is compensated by the load torque influence tending to a steady state offset which is compensated by the integrator. Once more having a relatively weak integrator in order to avoid large overshoots, convergence is obtained after some time (out of scale). Using the feed-forward term, the control action is load torque independent. The P-controller accelerates the machine to reference speed and its output goes to 0 while the feed-forward term continues to compensate the load torque.

5.2 Load Torque Step

In this section the ability of the observer to estimate the load torque is shown and the behavior of the modified controller during a load torque step should be compared with the one of a PI controller. For this reason a positive load torque step has been applied at constant machine speed. The results are shown in Fig. 8.

The load torque observer converges to the applied load torque after the step and the speed controller correct the speed variation which has been obtained due to the limited dynamic of the torque observer.

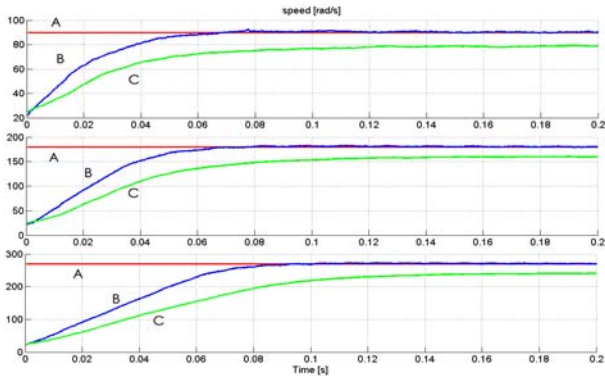


Fig. 6 Experimental result: speed reference steps 0rad/s to 90rad/s , 180rad/s , and 270rad/s (modulation index: $m = 0.29$, $m = 0.57$, and $m = 0.86$ respectively) with the constant load torque 3Nm (0.36pu) which are marked with the letter A. The results obtained with P controller with feed forward path are marked with B and the PI controller: C.

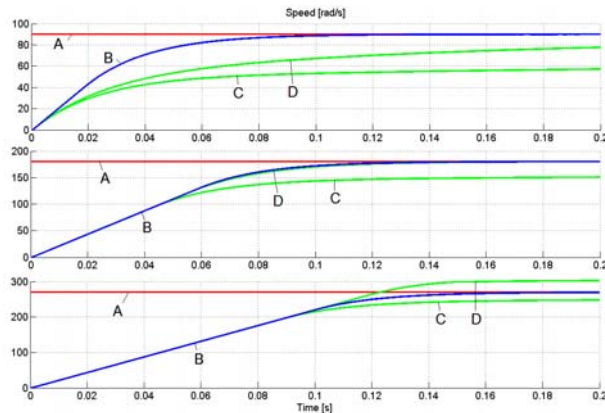


Fig. 7 Simulation result: speed reference steps 0rad/s to 90rad/s , 180rad/s , and 270rad/s (modulation index: $m = 0.29$, $m = 0.57$, and $m = 0.86$ respectively) with the constant load torque 3Nm (0.36pu). The reference speeds are marked with the letter A. The results obtained with P controller with feed forward path are marked with B. Furthermore a PI controller with two different integrator gains has been used: C standard, D aggressive with factor 5 between them.

Using a PI controller the controller acts and compensates the load torque, too. The proportional gain of the controller is used to compensate the load torque leading to a steady-state offset which must be compensated by integration. However, the gain of the integrator cannot be designed aggressive in order to avoid large overshoots and oscillations. For this reason it takes some time to compensate completely the load torque (out of scale in Fig. 8).

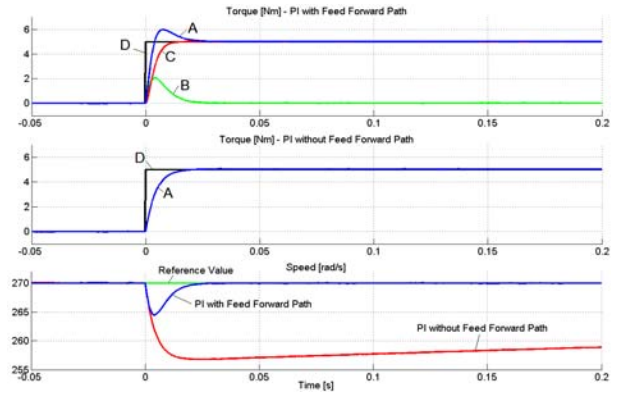


Fig. 8 Simulation result: load torque step 0Nm to 5Nm (0.61pu) at constant electrical speed 270rad/s (modulation index: $m = 0.86$) using the P controller with feed forward path and a PI controller. The torque and speed is shown for both cases, where A is the applied total electromagnetic torque T_e , B the torque which lead to a speed variation $T_{e\Delta\omega}$, C the compensated load torque T_{eT_l} , and D the applied load torque T_l .

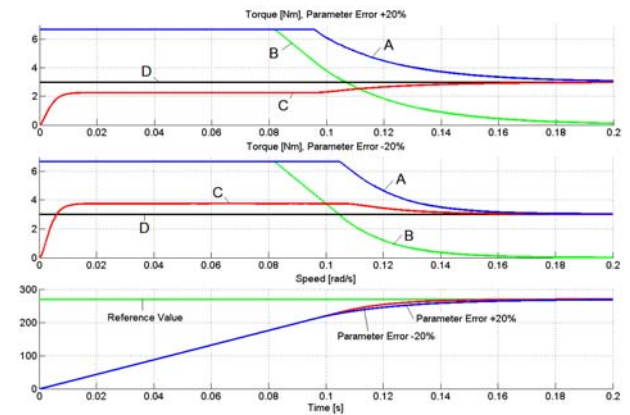


Fig. 9 Simulation result: speed reference steps 0rad/s to 270rad/s (modulation index: $m = 0.86$) with the constant load torque 3Nm (0.36pu). The torque and speed is shown for both cases, where A is the applied total electromagnetic torque T_e , B the torque which lead to a speed variation $T_{e\Delta\omega}$, C the compensated load torque T_{eT_l} , and D the applied load torque T_l .

5.3 Parameter Dependence

In order to show the influence of a parameter error, a positive and negative 20% error has been introduced on the value J/ψ . The results are shown in Fig. 9.

The parameter variation lead to a torque offset whether positive or negative depending of the sign of the parameter variation during transients and must be compensated by the speed controller. At steady-state

the offset is not observed. For this reason the torque compensator leads to benefits also in the case of parameter uncertainties if they are limited e.g. $\pm 20\%$.

6. Conclusion

Model Predictive Direct Current Control (MPDCC) has been designed for high power applications and has a high dynamics which can be compared to DTC. The modified speed controller with the load torque observer has been combined and tested with MPDCC in order to show a fairly simple possibility to further improve the dynamic behavior.

A feed-forward path can decouple the speed loop of a cascade control from the effects of the load torque, which is estimated with an observer, and comes along with two main advantages. In steady state the load torque lead to an offset if the speed controller and path whether do not have or have a weak integrative behavior which is desired in some systems in order to avoid overshoots and oscillations. An improvement brings a feed-forward path, which compensates the load torque with an electrical one setting a q -axis current. Moreover it improves also the dynamic behaviour of the speed controller. The load torque variations are detected and compensated, which lead to a small speed variations.

A drawback is the machine parameter dependence of the feed-forward path. Thus their accuracy influences directly the quality of the estimate. However, the error is limited to transients where the load torque is whether under- or overcompensated, i.e. it leads to a torque offset, which is compensated by the speed controller.

References

- [1] C.K. Kim, H.W. Rhew, Y.H. Kim, Robust speed control of PMSM using Kalman filter load torque observers, in: Proc. 23rd International Conference on Industrial Electronics, Control and Instrumentation IECON 97, Nov. 9-14, pp. 918-924.
- [2] S. Benaggoune, S. Belkacem, R. Abdessemed, Sensorless direct torque control of PMSM drive with EKF estimation of speed, rotor position and load torque observer, Asian Journal of Information Technology 6 (2) (2007) 236-242.
- [3] C. Khajorntraidet, J. Srisertpol, Torque control for DC servo motor using adaptive load torque compensation, in: 9th Wseas International Conference on System Science and Simulation in Engineering, 2010, pp. 254-258.
- [4] A. Goedel, I.N. Da Silva, P.J.A. Serni, A neural approach for load torque identification in electrical machinery, in: Proceedings of the WSEAS Int. Conf. on System Science, Applied Mathematics & Computer Science, and Power Engineering Systems, Rio De Janeiro, Brazil, 2002, pp. 2591-2596.
- [5] D.D. Neema, R.N. Patel, A.S. Thoke, ANN based flux and torque estimator for vector controlled induction drive with dynamic loading, International Journal of Computer and Electrical Engineering 1 (2) (2009) 245-250.
- [6] J.S. Ko, H. Kim, S.H. Yang, Precision speed control of PMSM using neural network disturbance observer on forced nominal plant, in: 5th Asian Control Conference, 2004, pp. 1746-1752.
- [7] K. Drobnič, M. Nemeč, D. Nedeljković, V. Ambrožič, Predictive direct control applied to AC drives and active power filter, IEEE Transactions on Industrial Electronics 56 (6) (2009) 1884-1893.
- [8] S. Kouro, P. Cortés, R. Vargas, U. Ammann, J. Rodríguez, model predictive control—A simple and powerful method to control power converters, IEEE Transactions on Industrial Electronics 56 (6) (2009) 1826-1838.
- [9] M. Pacas, J. Weber, Predictive direct torque control for the PM-synchronous machine, IEEE Transactions on Industrial Electronics 52 (5) (2005) 1350-1356.
- [10] J. Beerten, J. Verwecken, J. Driesen, Predictive direct torque control for flux and torque ripple reduction, IEEE Transactions on Industry Applications 57 (1) (2010) 404-412.
- [11] S. Bolognani, L. Peretti, M. Zigliotto, Design and implementation of model predictive control for electrical motor drives, IEEE Transactions on Industrial Electronics 56 (6) (2009) 1925-1936.
- [12] S. Mariethoz, A. Domahidi, M. Morari, Sensorless explicit model predictive control of permanent magnet synchronous motors, in: IEEE International Electric Machines and Drives Conference, 2009, pp. 1250-1257.
- [13] J.M. Maciejowski, Predictive Control with Constraints, Prentice Hall, 2002.
- [14] T. Geyer, G. Papafotiou, M. Morari, Model predictive direct torque control - part 1: Concept, algorithm, and analysis, IEEE Transactions on Industrial Electronics 56 (6) (2009) 1894-1905.
- [15] G. Papafotiou, J. Kley, K.G. Papadopoulos, P. Böhren, M. Morari, Model predictive direct torque control - part 2: Implementation and experimental evaluation, IEEE Transactions on Industrial Electronics 56 (6) (2009) 1894-1905.